Asian Journal of Chemistry; Vol. 35, No. 12 (2023), 3005-3012

ASIAN JOURNAL OF CHEMISTRY

https://doi.org/10.14233/ajchem.2023.30577

A Spectroscopic Approach on Permanganate Oxidation of 1-[(4-Chlorophenyl)methyl]piperidin-4-amine in Presence of Ruthenium(III) Catalyst with DFT Analysis on Reaction Mechanism Pathway

S. SHASHIDHAR[1,2], VIDYAVATI A. SHASTRY[2,*], SAMPATH CHINNAM[3], HAZEM ELKADY[4], DALAL Z. HUSEIN[5], ANUSUYA DEVI[1], K. GURUSHANTHA[3] and P.K. ASHA[1,*]

[1]Department of Chemistry, New Horizon College of Engineering (Affiliated to Visvesvaraya Technological University, Belgaum), Bengaluru-560103, India
[2]Department of Chemistry and Research in Chemistry, Visvesvaraya Technological University, SEA College of Engineering & Technology, Bangalore-560049, India
[3]Department of Chemistry, M.S. Ramaiah Institute of Technology (Affiliated to Visvesvaraya Technological University, Belgaum), Bengaluru-560054, India
[4]Department of Pharmaceutical Medicinal Chemistry & Drug Design, Faculty of Pharmacy (Boys), Al-Azhar University, Cairo11884, Egypt
[5]Department of Chemistry, Faculty of Science, New Valley University, El-Kharja 72511, Egypt

*Corresponding authors: E-mail: vidyavati_kinetic@yahoo.co.in; ashapkind@gmail.com

Received: 27 September 2023; *Accepted*: 26 October 2023; *Published online*: 2 December 2023; AJC-21462

The kinetic oxidation of 1-[(4-chlorophenyl)methyl]piperidin-4-amine (CMP) using alkaline potassium permanganate in presence of Ru(III) as catalyst was conducted spectrophotometrically at 303 K. The Pseudo first-order reaction was maintained with regard to oxidant and substrate during the reaction at an ionic strength of 0.01 mol dm^{-3}. The first-order kinetics has been depicted with respect to catalyst Ru(III) chloride and less than unit order with substrate and medium. For the slow step, different activation parameters including $\Delta H^{\#}$ (kJ mol^{-1}), E_a (kJ mol^{-1}), $\Delta G^{\#}$ (kJ mol^{-1}) and $\Delta S^{\#}$ (J K^{-1} mol^{-1}) were calculated. The effect of temperature, variation of substrate concentration, oxidant, ionic strength were studied. The stoichiometry ratio of the reaction to the substrate and oxidizing agent was found to be 1:4. The products of reaction were isolated and identified as chlorobenzene and L-alanine, N-(2-aminomethylethyl)-carboxylic acid by LC-MS spectra, a suitable mechanism has been proposed and the rate laws are derived. The frontier molecular orbital (FMO) and frontier electron density (FED) of piperidiamine and the oxidative products were studied using density functional theory (DFT). The results of the theoretical calculations supported the suggested reaction pathways.

Keywords: Kinetics, 1-[(4-Chlorophenyl)methyl]piperidin-4-amine, Mechanism, Rate law, Oxidation, Potassium permanganate.

INTRODUCTION

Permanganate serves as an exclusive oxidizing agent in every pH medium [1] in the field of synthetic and analytical chemistry. According to Insauti *et al*. [2], it has several advantages due to its strong, intensely coloured serving as self-indicator. Manganese ions in permanganate ion shows various oxidation states from +2 to +7, making it a good oxidizing agent. Manganate ion, MnO_4^{2-} is the stable reduction product in strong alkaline medium [3-5]. This oxidant finds a major application in organic synthesis [6-8] exclusively after the initiation of phase transfer catalysis. Various biological molecule like amino acids [9], nucleic acid [10], oxidation is already reported, where the various oxidation states of manganese have been defined. The active species $MnO_4(OH)^{2-}$ forms intermediate complex on reacting with the substrate then the complex decompose into product in mojority of the cases [11].

Substituted piperidin-4-amine derivatives exhibited as antifungal, antihistaminic, antimicrobial [12,13], antitubercular, anthelmintic, antipsychotic agents [13] as these derivatives are versatile ring systems and well established medicinally useful class of compounds. Piperidin-4-amine derivatives are used as cognition enhancing drugs [14] and anticancer medicines include pyrimidine derivatives with piperidin-4-amine linkage [15].

Ruthenium(III) is a well-known catalyst for redox reactions in alkaline environments [16,17]. The rapid kinetics of reactions between RuO_4, ruthenate(VII), manganite(VI) and MnO_4^{2-}, have been investigated [18] and it is anticipated that the reaction will proceed *via* an outer-sphere mechanism. There occurs continuous exchange between MnO_4^- and MnO_4^{2-} which has been studied in detail. The present study focuses on the significance of 4-piperidiamine in medicine and aims to investigate the mechanisms and stability of the reaction product using density functional theory. Specifically, the catalyzed oxidation of 1-[(4-chlorophenyl)methyl]piperidin-4-amine (CMP) by permanganate ion in a strongly aqueous basic medium has been examined

EXPERIMENTAL

Chemicals used in the study were of analytical reagent quality and the solutions were prepared in double-distilled water. Freshly prepared potassium permanganate ($KMnO_4$) solution was standardized using Systronic UV-visible spectrophotometer at 525 nm. Ruthenium(III) chloride [$RuCl_3 \cdot xH_2O$] purchased from VASA Scientific Center, Bangalore, India was used without further purification and the solution was standardized as according to the earlier methods [19].

The required amount of sample was dissolved in 1 mL of 1 N NaOH and the solution was then diluted with distilled water to prepare 1-[(4-chlorophenyl)methyl]piperidin-4-amine (CMP). The NaOH and KNO_3 solutions were also prepared in double-distilled water and standardized according to established procedures.

The theoretical DFT calculations were performed using Gaussian09 package then the output files were visualized and analyzed using GaussView 0.5 and GaussSum.

Kinetic studies: With [CMP] > [$KMnO_4$], 10:1 in the presence of Ru(III) catalyst, at constant ionic strengh of 0.1 mol dm^{-3}, the kinetics of oxidation of CMP were studied spectrophotometrically under pseudo-first order conditions. While the concentration of ruthenium(III) ranged from 1.5×10^{-6} to 25×10^{-6} mol dm^{-3}, the CMP concentration ranged from 0.5×10^{-3} to 5×10^{-3} mol dm^{-3}. Between 2.5×10^{-3} and 0.02 mol dm^{-3} of NaOH was regulated. The Beer's law for potassium permanganate at 525 nm, had previously been confirmed [20], giving $\varepsilon = 2390.5$ dm^3 mol^{-1} cm^{-1} (literature $\varepsilon = 2400$ dm^3 mol^{-1} cm^{-1}).

By monitoring the disapperance of manganese(VII) at λ_{max} = 525 nm with systronics made UV-visible spectrophotometer equipped with a themostatic reservoir for temperature control with an accuracy of 0.1 ºC, the reaction kinetics were asertained. The pseudo-first order rate constants (k_{obs}) were determined by calculating the slope of log (absorbance) against time in seconds.

RESULTS AND DISCUSSION

Analysis of product with stoichiometry: Reaction mixtures in various ration of [MnO_4^-] > [CMP] were prepared, each containing different ratios of the reactants in the presence of Ru(III) of concentration 5×10^{-6} mol dm^{-3}, a reaction duration of 24 h was maintained by keeping the media and ionic strength constant.

To complete the reaction, the prepared reaction mixtures were left to stand at 298 K. Spectrophotometric analysis was performed on the residual MnO_4^-. According to eqn. 1, three moles of MnO_4^- interacted with one mole of CMP.

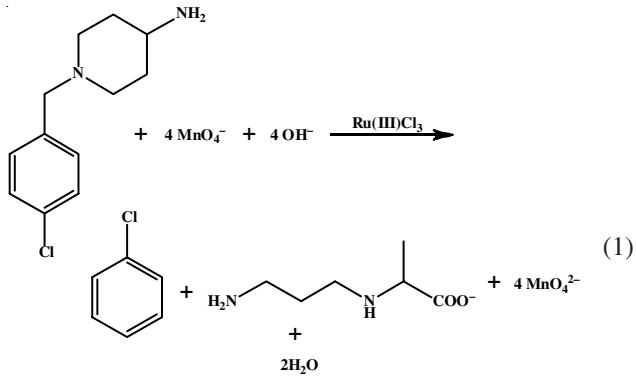

(1)

Liquid chromatography-mass spectra (LC-MS) technique was used to identify the product (Fig. 1). The result is L-alanine, N-(2-amino methylethyl)-carboxylic acid, as seen by the peak near 147. Presence of chlorobenzene is indicated by at peak 112.

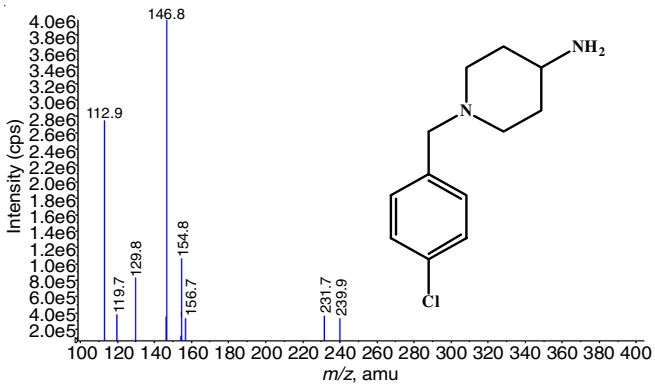

Fig. 1. LC-MS of product analysis of $KMnO_4$ oxidation of 1-[(4-chlorophenyl)methyl]piperidin-4-amine in alkaline medium in presence of Ru(III) catalyst

Effect of potassium permanganate: While the concentration of the other reactants remained constant, potassium permanganate concentration was modulated from 0.5×10^{-4} to 5×10^{-4} mol dm^{-3}. A first-order dependency with the oxidant was seen when the beginning rates were plotted against potassium permanganate concentration.The unit order for $KMnO_4$ is determined by the constant values of k (Table-1).

Effect of 1-[(4-chlorophenyl)methyl]piperidin-4-amine: The concentration of CMP was varied from 0.5×10^{-3} to 5×10^{-3} mol dm^{-3} by maintaining concentrations of other reactants were held constant, the fractional order dependence with substrate has be observed in the initial rates *vs*. CMP concentration.

Effect of sodium hydroxide (medium): Sodium hydroxide concentration was modulated from 2.5×10^{-3} to 0.02 mol dm^{-3} while maintaining consistent concentration of all other reactants. The rate increased as NaOH concentration increased. Initial rates *versus* NaOH concentration illustrate the order less than unit.

TABLE-1
EFFECTS ON REACTION RATE OF 1-[(4-CHLOROPHENYL)METHYL]PIPERIDIN-4-AMINE, [$KMnO_4$], [OH^-] AND [Ru(III)] AT 30 °C, I = 0.01 mol dm^{-3}

$[MnO_4^-] \times 10^4$ (M)	[CMP] × 10^3 (M)	[OH^-] (M)	[NO_3^-] (M)	[Ru(III)] × 10^6 (M)	$k_{obs} \times 10^2$ (s^{-1})	$k_{cal} \times 10^2$ (s^{-1})
0.5	2.5	0.0100	0.0010	5.0	1.32	1.43
1.5	2.5	0.0100	0.0010	5.0	1.32	1.43
2.5	2.5	0.0100	0.0010	5.0	1.39	1.43
3.5	2.5	0.0100	0.0010	5.0	1.31	1.43
5.0	2.5	0.0100	0.0010	5.0	1.36	1.43
2.5	0.5	0.0100	0.0010	5.0	0.45	0.43
2.5	1.5	0.0100	0.0010	5.0	0.92	1.04
2.5	2.5	0.0100	0.0010	5.0	1.39	1.43
2.5	3.5	0.0100	0.0010	5.0	1.85	1.72
2.5	5.0	0.0100	0.0010	5.0	2.55	2.01
2.5	2.5	0.0025	0.0010	5.0	0.58	0.56
2.5	2.5	0.0050	0.0010	5.0	1.10	0.94
2.5	2.5	0.0100	0.0010	5.0	1.39	1.43
2.5	2.5	0.0150	0.0010	5.0	1.75	1.74
2.5	2.5	0.0200	0.0010	5.0	2.13	1.94
2.5	2.5	0.0100	0.0025	5.0	1.29	1.43
2.5	2.5	0.0100	0.0050	5.0	1.32	1.43
2.5	2.5	0.0100	0.0010	5.0	1.39	1.43
2.5	2.5	0.0100	0.0020	5.0	1.47	1.43
2.5	2.5	0.0100	0.0030	5.0	1.56	1.43
2.5	2.5	0.0100	0.0010	1.5	0.47	0.43
2.5	2.5	0.0100	0.0010	2.5	0.97	0.71
2.5	2.5	0.0100	0.0010	5.0	1.39	1.43
2.5	2.5	0.0100	0.0010	10.0	2.57	2.87
2.5	2.5	0.0100	0.0010	25.0	8.53	7.19

Temperature effect: The rates of reaction were examined at 303, 308, 313, 318 and 323 K [21]. The slopes of the log A *versus* time graphs were utilized to determine slow step of rate constants (k) of reaction mechanism. The rate of chemical reactions is accelerated by temperature and the values are given in Table-2.

TABLE-2
RATE CONSTANT FOR CMP OXIDATION BY $KMnO_4$ IN AQUEOUS ALKALINE MEDIUM IN WITH Ru(III) CATALYST AT VARIOUS TEMPERATURES

Temperature (K)	$k \times 10^2$ (s^{-1})
303	1.43
308	1.83
313	2.65
318	3.25
323	5.58

Effect of catalyst ruthenium: Keeping the concentrations of the other reactants constant at [substrate] = 2.5×10^{-3}, [oxidant] = 2.5×10^{-4} and [OH^-] = 0.01 mol dm^{-3}, the reaction was examined by increasing the catalyst concentration from 1.5×10^{-6} to 25×10^{-6} mol dm^{-3}. The rate of raction was directly varies with concentration of Ru(III) indicating unit order.

Polymerization study: Addition of acrylonitrile (monomer) Ru(III) catalyzed processes, followed by 2 h period of inert storage, was used to monitor the oxidation of CMP by $KMnO_4$ [22]. After 2 h, the reaction mixtures were diluted with methanol to form white precipitate, showing free-radical intervention, concluding that the reaction follows an radical mechanism (**Scheme-I**).

$$MnO_4^- + OH^- \underset{}{\overset{K_1}{\rightleftharpoons}} [MnO_4OH]^{2-}$$

$$\text{Substrate} + [Ru(H_2O)_5OH]^{2+} \overset{K_2}{\rightleftharpoons} \text{Complex} + H_2O$$

$$\text{Complex} + [MnO_4OH]^{2-} \xrightarrow[\text{Slow}]{k} \text{Products} + [Ru(H_2O)_4OH]^{2+} + H_2O$$

Scheme-I

In presence of alkaline medium permanganate ion behaves as a good oxidizing agent, exhibiting number of oxidation states. For pH > 12, the reaction product is Mn(VI). The oxidant has first order kinetics has been depicted with respect to catalyst Ru(III) chloride, the substrate and alkali has fractional order dependence.

In alkaline medium permanganate exhibits different oxidation states [23], which observed during the reaction *i.e.*, colour changes violet to blue and further green. $KMnO_4$ changes its colour from viloet Mn(+7) to dark green Mn(+6) through Mn(+4) ion which is blue.

The presence of hydrated form of ruthenium(III) chloride in alkaline media as $[Ru(H_2O)_6]^{3+}$ have been reported [24]. The oxidation reaction between CMP and permanganate in existance of Ru(III) chloride has stoichiometry of 1:4 with unit order dependence on permangate and Ru(III) and fraction order dependance on base and CMP, which indicates the formation of $MnO_4 \cdot OH^{2-}$, it is further supported by the plot [Ru(III)]/k_{obs} *vs.* 1/[OH^-] with positive intercept. Based on the above observed orders with respect to oxidant, catalyst and reductant and OH^-, a suitable mechanism involving radical formation can be proposed. In this case, hydrated species of Ru(III) reacts with the CMP to

give complex (C2), this on combines with unit mole of alkaline $KMnO_4$ in rate determining step to form free radical derived from CMP and MnO_4^{2-} with the regeneration of catalyst. The formation of complex C2 is further supported by earlier works [25] with fractional order of OH^- and reductant. The free radical consumes three more moles of alkaline permangate to yield product in the successive steps as in Fig. 2. The activation parameters calculations for the reaction's enthalpy, entropy and free energy from the vant Hoffs plot and tabulated in Table-3. The electron transfer process was supported by moderate values of these parameters. The high negative value of entropy suggest the complex is more disordered than CMP.

TABLE-3
ACTIVATION PARAMETERS DATA OF $KMnO_4$ OXIDATION OF CMP IN AQUEOUS ALKALINE MEDIUM WITH Ru(III) CATALYST

Activation parameters	Values
$\Delta H^{\#}$ (kJ mol^{-1})	51.07
E_a (kJ/mol)	53.5
$\Delta G^{\#}$ (kJ mol^{-1})	84.6
$\Delta S^{\#}$ (J K^{-1} mol^{-1})	-112.72
Log A	7.3

The rate law for the above proposed mechanism can be eloborated in **Scheme-II**.

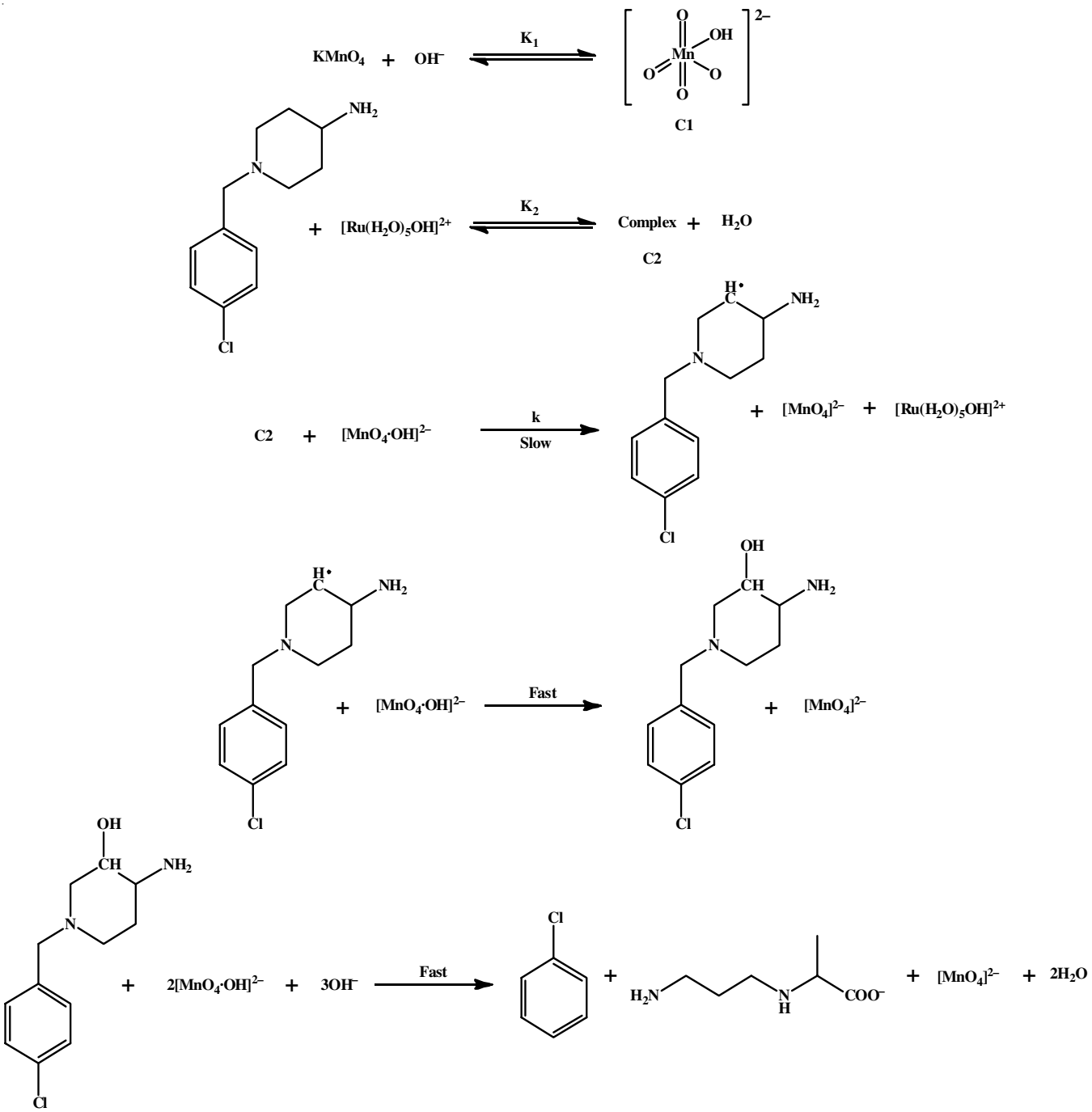

Fig. 2. Mechanism of catalyzed reaction involving slow step, intermediate and fast steps

$$\text{Rate} = \frac{-d[MnO_4^-]}{dt} = k_1K_1K_2[MnO_4^-][OH^-][CMP][Ru(III)] \quad (2)$$

$$[CMP]_t = [CMP]_f + [\text{Complex } (C_2)]$$
$$= [CMP]_f + K_2[Ru(III)]_f[CMP]_f$$

$$[CMP]_f = \frac{[CMP]_t}{1 + K_2[Ru(III)]_f} \quad (3)$$

Similarly, the total $[OH^-]$ can be written as:

$$[OH^-]_t = [OH^-]_f + \text{Complex } (C_2)$$
$$= [OH^-]_f + K_1[MnO_4^-]_f[OH^-]_f$$

$$[OH^-]_f = \frac{[OH^-]_t}{1 + K_1[MnO_4^-]_f} \quad (4)$$

$$[Ru(III)]_t = [Ru(III)]_f + [\text{Complex } (C_2)]$$
$$= [Ru(III)]_f + K_2[Ru(III)]_f[CMP]_f$$

$$[Ru(III)]_f = \frac{[Ru(III)]_t}{1 + K_2[CMP]_f} \quad (5)$$

Similarly,

$$[MnO_4^-]_f = \frac{[MnO_4^-]_t}{1 + K_1[OH^-]_f} \quad (6)$$

Put eqns. 3-6 in eqn. 2, then

$$\text{Rate} = \frac{d[MnO_4^-]}{dt} = \frac{k_1K_1K_2[CMP]_t[MnO_4^-]_t[Ru(III)]_t[OH^-]_t}{\{1 + K_2[Ru(III)]_f\}\{1 + K_1[OH^-]\} + \{1 + K_1[MnO_4^-]_f\}\{1 + K_2[CMP]_f\}} \quad (7)$$

Due to low concentration of ruthenium and permanganate the terms $\{1 + K_2[Ru(III)]_f\}$ and $\{K_1[MnO_4^-]_f\}$ can be omitted. On neglecting total and free (t and f), eqn. 7 becomes:

$$\frac{\text{Rate}}{[MnO_4^-]} = k_{obs} = \frac{k_1K_1K_2[CMP][Ru(III)][OH^-]}{1 + K_2[CMP] + k_1[OH^-] + K_1K_2[CMP][OH^-]} \quad (8)$$

On rearranging the above equation:

$$\frac{[Ru(III)]}{k_{obs}} = \frac{1}{k_1K_1K_2[CMP][OH^-]} + \frac{1}{kK_1[OH^-]} + \frac{1}{kK_2[CMP]} + \frac{1}{k} \quad (9)$$

Scheme-II

The plots of $[Ru(III)]/k_{obs}$ *vs.* $1/[CMP]$ and $[Ru(III)]/k_{obs}$ *vs.* $1/[OH^-]$ (Fig. 3) are linear with intercepts shows the complex formation of Ru(III)-CMP. The slope and intercept of the aforementioned plots are used to derive the values of k, K_1 and K_2 as 14.1×10^2 dm^3 mol^{-1} s^{-1}, 91.9 dm^3 mol^{-1} and 2.97×10^2 dm^3 mol^{-1}, respectively. These values are used to calculate the rate constants under different experimental circumstances and to compare the results obtained during experiment, which were in good agreement.

DFT and FMO studies: To understand the energy level and stability of reactant and product, the molecular geometry of the 27RR medication was optimized using the Gaussian 09 program using density functional theory (DFT) and the B3LYP/6-311G++(d,p) method.

The optimized structures of both reactant and product are shown in Fig. 4a-b. The calculated ground (total) energy and dipole moment for reactant and product were found to be (-28229.0 e. V and 1.505 Debye) and (-18828.496 e. V and 1.859 Debye), respectively. The product is more electronegative than the reactant based on the calculated Dm value as the charge separation in bonded atoms in chlorobenzene is greater. The transfer of one electron from the HOMO level to the LUMO state best describes electronic absorption, which describes the shift from the initial stae to the first excited state. The energies of frontiers orbitals (HOMO and LUMO) play a significant effect on chemical reactivity, according to frontier molecular orbital theory. The global chemical reactivity parameters of a molecule are all correlated with the HOMO-LUMO gap [26, 27]. High chemical reactivity and low kinetic stability are caused by a small LUMO-HOMO gap. The narrow HOMO-LUMO gap is significant for poor chemical stability because it is energitically favour to tranfer electron to a high-lying LUMO and/

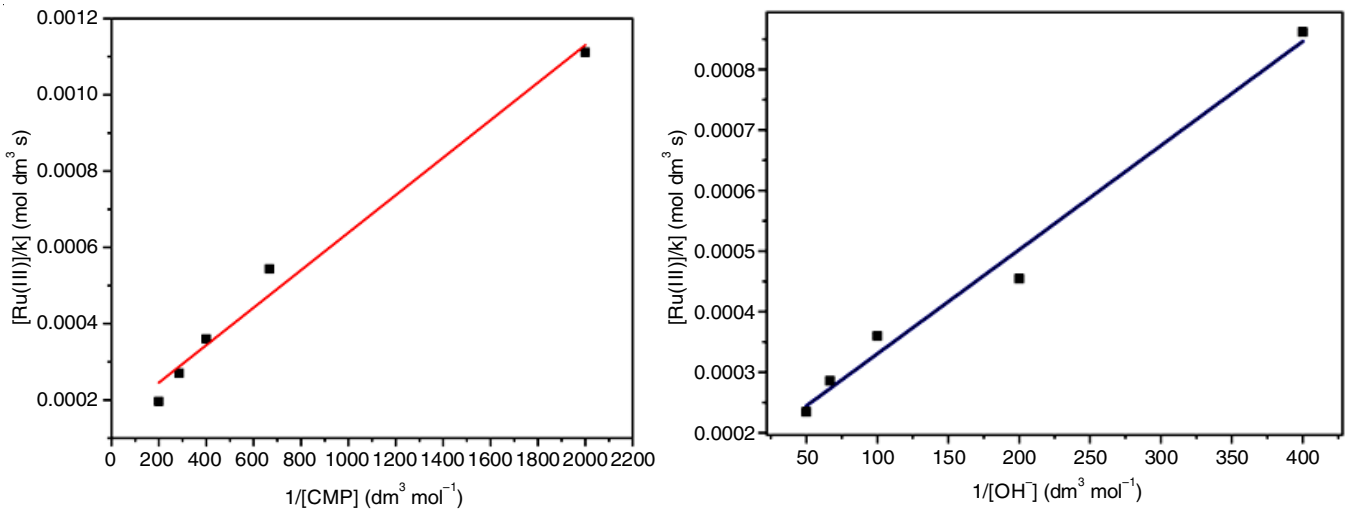

Fig. 3. Linear plots $[Ru(III)]/k_{obs}$ *vs.* $1/[CPB]$ and $[Ru(III)]/k_{obs}$ *vs.* $1/[OH^-]$ showing the rate-law validity of catalyzed reaction

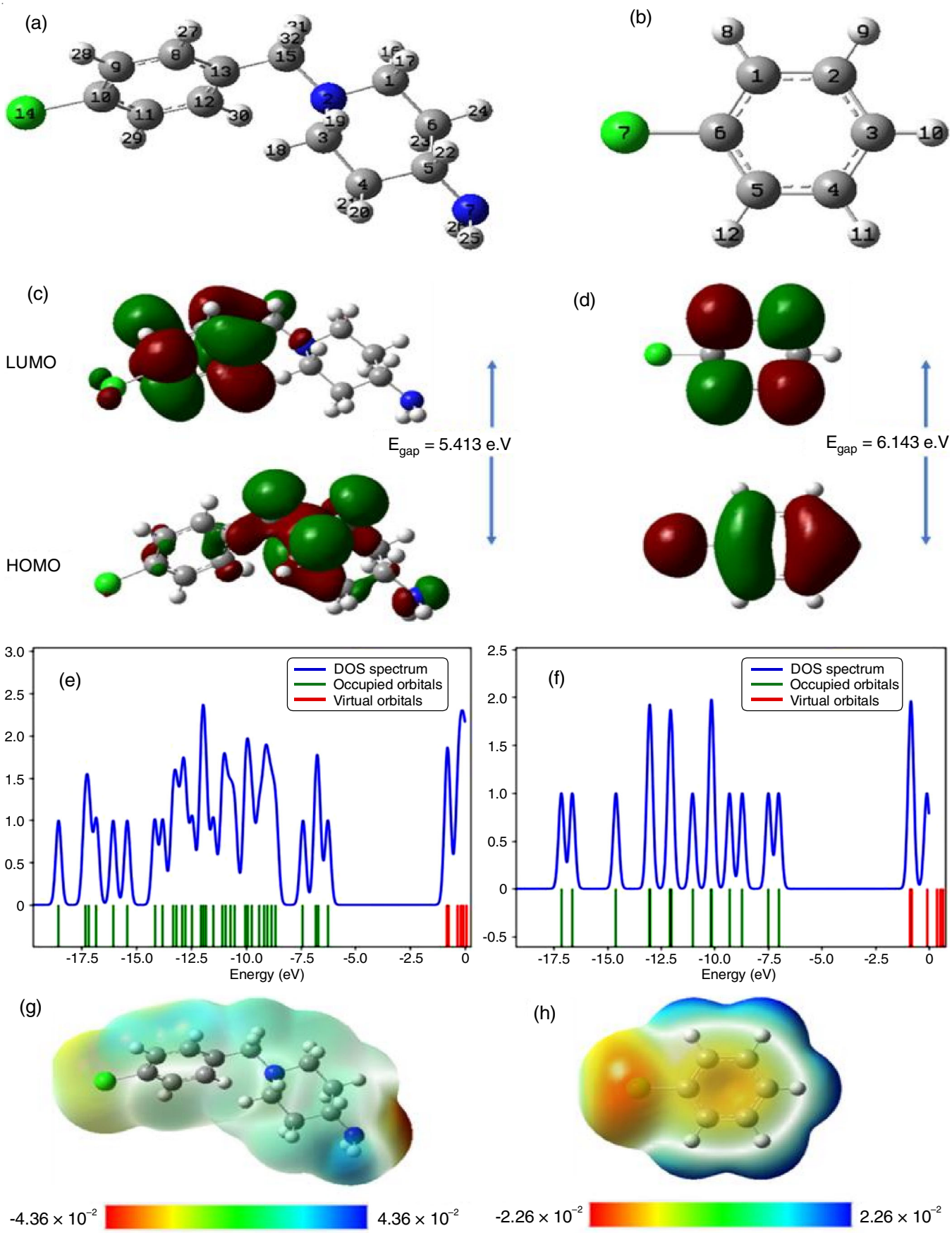

Fig. 4. Optimized geometry (a,b), the frontier molecular orbitals (c,d), the total density of state (e,f) and the electrostatic potential map (g,h) at B3LYB/6-311+G(d,p) for the reactant and the product

TABLE-4
DFT CALCULATED GLOBAL REACTIVITY PARAMETERS FOR THE REACTANT AND PRODUCT. THE CHEMICAL POTENTIAL (μ), SOFTNESS (σ), ELECTRON AFFINITY (EA), ELECTRONEGATIVITY PARAMETER (χ), HARDNESS (η), ELECTROPHILIC INDEX (ω) AND MAXIMAL CHARGE ACCEPTANCE (ΔN_{max}) OF REACTANT AND PRODUCT, AS WELL AS THEIR HOMO AND LUMO ENERGY GAPS (E_{gap})

Parameter	IP	EA	μ (eV)	χ (eV)	η (eV)	σ (eV)	ω (eV)	Dm (Debye)	TE (eV)	ΔN_{max}	ΔE (eV)
Reactant	6.256	-0.84	-3.55	3.55	2.70	0.36	17.05	1.505	-28229.0	1.31	-17.05
Product	7.007	0.86	-3.93	3.93	3.07	0.32	23.78	1.859	-18828.4	1.28	-23.78

or remove them from a low lying HOMO in any potential reaction.

The HOMO-LUMO gap for the reactant in the present study is 5.41 e. V, Fig. 4c and Table-4, whereas the product chlorobenzene has the highest energy gap (6.14 e. V) and the lowestsoftness (0.32 eV), which may help explain why it is more stable than the reactant.

Computational calculations: The molecular electrostatic potential (MESP) was utilized to predict the reactive regions that would be susceptible to electrophilic and nucloephilic attacks, which supports the understanding of biological systems and interactions [28-30]. The coloured shades of red indicate negative potential and are ready for electrophilic attack while the shades of blue indicate positive potential and are ready for the nucleophilic attack. Based on the above observations, the probable hydrated ruthenium and the CMP probable complex (C2) structure are shown in Fig. 5.

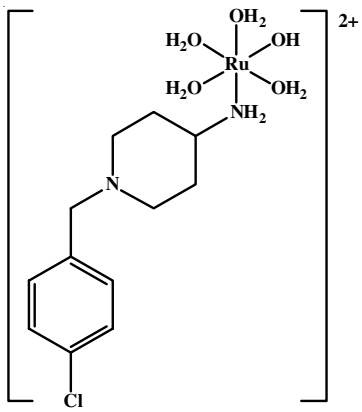

Fig. 5. Probable complex formation between Ru(III) and CMP

The preference of CMP to form complexes with hydrated ruthenium instead of alkaline permanganate can be attributed to the combination of low ionization energy and electrophilic index. In this context, the low ionization energy of CMP makes it more inclined to undergo complexation reactions with hydrated ruthenium. On the other hand, the electrophilic index of alkaline permanganate is not significant enough to facilitate nucleophilic assault, thereby reducing its ability to form complexes. The low hardness of CMP facilitates the formation of complexes for enhanced stability. The product chlorobenzene has a greater dipole moment than CMP, which enhances the stability of product.

Conclusion

The spectroscopic kinetic oxidation of analysis of 1-[(4-chlorophenyl)methyl]piperidin-4-amine (CMP) by $KMnO_4$ in the presence of ruthenium(III) as catalyst was carried out at 300 K and a wavelength of 525 nm. The stoichiometry of the reaction was determined to be 1:4 and the end products were L-alanine, N-(2-aminomethylethyl)-carboxylic acid and chlorobenzene. A suitable mechanism was proposed based on the experimental results. To support the stability of the product and reaction pathway, DFT investigations on reactant and product were conducted.

ACKNOWLEDGEMENTS

The authors are grateful to New Horizon College of Engineering, Bangalore and SEA College of Engineering and Technology, Bangalore, India for providing the support.

CONFLICT OF INTEREST

The authors declare that there is no conflict of interests regarding the publication of this article.

REFERENCES

1. M.C. Day and J. Selbin, *Theoretical Inorganic Chemistry*. Reinhold Publishing Corporation, New York, 344 (1985).
2. M.J. Insausti, F. Mata-PÉRez and M.P. Alvarez-Macho, *Int. J. Chem. Kinet.*, **27**, 507 (1995); https://doi.org/10.1002/kin.550270509
3. G. Fang, C. Zhu, M. Chen, J. Zhou, B. Tang, X. Cao, X. Zheng, A. Pan and S. Liang, *Adv. Funct. Mater.*, **29**, 1808375 (2019); https://doi.org/10.1002/adfm.201808375
4. L.I. Simandi, M. Jaky, C.R. Savage and Z.A. Schelly, *J. Am. Chem. Soc.*, **107**, 4220 (1985); https://doi.org/10.1021/ja00300a023
5. S. Nadimpalli, R. Rallabandi and L.S. Dikshitulu, *Transition Met. Chem.*, **18**, 510 (1993); https://doi.org/10.1007/BF00136616
6. S.A. Farokhi and S.T. Nandibewoor, *J. Indian Chem. Soc.*, **93**, 427 (2016).
7. A.A.P. Khan, A. Mohd, S. Bano, A. Husain and K.S. Siddiqi, *Transition Met. Chem.*, **35**, 117 (2010); https://doi.org/10.1007/s11243-009-9303-z
8. P.N. Naik, S.A. Chimatadar and S.T. Nandibewoor, *Ind. Eng. Chem. Res.*, **48**, 2548 (2009); https://doi.org/10.1021/ie801633t
9. D. Laloo and M.K. Mahanti, *J. Phys. Org. Chem.*, **3**, 799 (1990); https://doi.org/10.1002/poc.610031205
10. V.K. Sharma and N.J. Graham, *Ozone Sci. Eng.*, **32**, 81 (2010); https://doi.org/10.1080/01919510903510507
11. R.M. Mulla, G.C. Hiremath and S.T. Nandibewoor, *J. Chem. Sci.*, **117**, 33 (2005); https://doi.org/10.1007/BF02704359
12. L. Jean, I. Baglin, J. Rouden, J. Maddaluno and M.-C. Lasne, *Tetrahedron Lett.*, **42**, 5645 (2001); https://doi.org/10.1016/S0040-4039(01)00985-6
13. M. Manish, M.S. Suraj, M.S. Ramesh, G. Vidyasagar and S. Birendra, *J. Chem. Pharm. Res.*, **3**, 766 (2011).

14. D. Manetti, E. Martini, C. Ghelardini, S. Dei, N. Galeotti, L. Guandalini, M.N. Romanelli, S. Scapecchi, E. Teodori, A. Bartolini and F. Gualtieri, *Bioorg. Med. Chem. Lett.*, **13**, 2303 (2003); https://doi.org/10.1016/S0960-894X(03)00437-2
15. M.S.R. Gangireddy, M. Mantipally, V.N. Badavath, V.C. Maddipati, K. Paidikondala, N.K. Katari and R. Gundla, *Chem. Data Coll.*, **32**, 100646 (2021); https://doi.org/10.1016/j.cdc.2021.100646
16. H.V. Rajeshwari, A.P. Savanur, S.T. Nandibewoor and S.A. Chimatadar, *J. Indian Chem. Soc.*, **87**, 295 (2010).
17. A.K. Singh, B. Jain, R. Negi, Y. Katre, S.P. Singh and V.K. Sharma, *Transition Met. Chem.*, **35**, 407 (2010); https://doi.org/10.1007/s11243-010-9342-5
18. L. Jattinagoudar, S. Nandibewoor and S. Chimatadar, *J. Solution Chem.*, **45**, 497 (2016); https://doi.org/10.1007/s10953-016-0455-0
19. J. Scherzer and L.B. Clapp, *J. Inorg. Nucl. Chem.*, **30**, 1107 (1968); https://doi.org/10.1016/0022-1902(68)80331-8
20. E.B. Elkaeed, R.G. Yousef, H. Elkady, I.M. Gobaara, B.A. Alsfouk, D.Z. Husein, I.M. Ibrahim, A.M. Metwaly and I.H. Eissa, *Molecules*, **27**, 4606 (2022); https://doi.org/10.3390/molecules27144606
21. K.S. Ravindra, V.A. Shastry, S. Shashidhar and M. Kumar, *Physical Chem. Res.*, **11**, 865 (2023); https://doi.org/10.22036/PCR.2022.361486.2191
22. M.D. Meti, M.H. Lamani, A.G. Naikar, S.S. Sutar, S.T. Nandibewoor and S.A. Chimatadar, *Monatsh. Chem.*, **146**, 1485 (2015); https://doi.org/10.1007/s00706-015-1410-2
23. M. Patgar, S. Nandibewoor and C. Shivamurti, *Phys. Chem. Commun.*, **3**, 52 (2016).
24. P.A. Magdum, A.M. Bagoji and S.T. Nandibewoor, *J. Phys. Org. Chem.*, **28**, 743 (2015); https://doi.org/10.1002/poc.3478
25. S.B. Konnur and S.T. Nandibewoor, *Russ. J. Phys. Chem. A. Focus Chem.*, **93**, 1686 (2019); https://doi.org/10.1134/S003602441909022X
26. T. Wang and D.Z. Husein, *Environ. Sci. Pollut. Res. Int.*, **30**, 8928 (2022); https://doi.org/10.1007/s11356-022-20050-2
27. M.S. Taghour, H. Elkady, W.M. Eldehna, N. El-Deeb, A.M. Kenawy, E.B. Elkaeed, B.A. Alsfouk, M.S. Alesawy, D.Z. Husein, A.M. Metwaly and I.H. Eissa, *PLoS One*, **17**, e0272362 (2022); https://doi.org/10.1371/journal.pone.0272362
28. D.Z. Husein, R. Hassanien and M. Khamis, *RSC Adv.*, **11**, 27027 (2021); https://doi.org/10.1039/D1RA04754J
29. E.B. Elkaeed, R.G. Yousef, H. Elkady, A.A. Alsfouk, D.Z. Husein, I.M. Ibrahim, M. Alswah, H.S. Elzahabi, A.M. Metwaly and I.H. Eissa, *Processes*, **10**, 2290 (2022); https://doi.org/10.3390/pr10112290
30. R.G. Yousef, H. Elkady, E.B. Elkaeed, I.M. Gobaara, H.A. Al-Ghulikah, D.Z. Husein, I.M. Ibrahim, A.M. Metwaly and I.H. Eissa, *Molecules*, **27**, 7719 (2022); https://doi.org/10.3390/molecules27227719